Analyst

ROYAL SOCIETY OF CHEMISTRY

PAPER

View Article Online
View Journal | View Issue

Cite this: *Analyst*, 2025, **150**, 1807

Encapsulating Cu NCs with aggregation-induced emission into metal–organic framework ZIF-8 as a novel fluorescent nanoprobe for the highly sensitive detection of felodipine†

Juan Du, Huixiao Tong, Jinwen Chen, Qikun Zhang and Shenghua Liao *

Fluorescent metal–organic framework nanocomposites (f-MOFs) have been gaining increasing attention in the fields of chemosensors and biosensors due to their unique signal amplification mechanisms and improved selectivity. However, most f-MOFs are constructed by encapsulating fluorescent labelling agents into frameworks *via* host–guest interactions. The notorious aggregation-caused quenching effect of these fluorescent labelling agents often leads to a decreased fluorescent quantum yield in f-MOFs. Herein, a novel fluorescent nanocomposite, Cu NCs@ZIF-8, was designed and prepared by encapsulating copper nanoclusters (Cu NCs) with aggregation-induced emission (AIE) effects into zeolitic imidazolate framework ZIF-8 through electrostatic attraction. Owing to the AIE effect of Cu NCs and the spatial confinement of ZIF-8, the intramolecular motion of surface ligand hydrolipidic acid (DHLA) in Cu NCs was restricted, resulting in the formation of a highly emissive nanocomposite, Cu NCs@ZIF-8. Intriguingly, the UV-Vis absorption spectrum of felodipine overlaps with the excitation spectrum of Cu NCs@ZIF-8. Therefore, a novel fluorescent nanoprobe based on Cu NCs@ZIF-8 was developed for the highly sensitive detection of felodipine *via* the inner-filtration effect mechanism. Under optimal detection conditions, the linear response range of Cu NCs@ZIF-8 for felodipine was found to be 1–25 μM, with a detection of limit of 0.09 μM. While determining the labelling-amount percentage in commercially available felodipine tablets, the experimental results validated that the proposed Cu NCs@ZIF-8 nanoprobe exhibits good selectivity and excellent accuracy. This expands the potential applications of fluorescent metal–organic frameworks encapsulated with metal nanoclusters exhibiting AIE properties, positioning them as fluorescent nanoprobes for pharmaceutical quality control.

Received 4th December 2024,
Accepted 24th March 2025

DOI: 10.1039/d4an01506a

rsc.li/analyst

Introduction

As an emerging novel functional material, metal–organic frameworks (MOFs) consist of secondary building units (such as metal ions[1] or metal clusters[2]) and organic linkers, forming expanded crystalline frameworks. Due to their large specific surface area, tunable porosity, facile synthesis, and tailorable physicochemical properties,[3] MOFs offer significant advantages in a wide range of fields, including gas storage,[4] catalysis,[5] and chemical sensing.[6]

Recently, increasing attention has been focused on the synthesis and application of fluorescent metal–organic frameworks nanocomposites (f-MOFs).[7] During the construction of f-MOFs, MOFs are commonly used as carriers for encapsulating various fluorescent nanomaterials, such as quantum dots,[8] carbon dots,[9] up-conversion nanoparticles,[10] among others.[11] However, it is worth noting that these fluorescent nanomaterials often exhibit a notorious phenomenon known as the aggregation-caused quenching (ACQ) effect,[12] which leads to decreased photoluminescence quantum yields (QY) in f-MOFs compared to those of individual fluorescent nanomaterials, thereby hindering advancements in the resolution of f-MOFs. Therefore, research has increasingly focused on the development of f-MOFs exhibiting aggregation-induced emission (AIE) properties, making this a current area of growing research interest.[13–15]

It is well-known that f-MOFs presenting the AIE effect are constructed either by using organic linkers with AIE properties as building units[16] or by encapsulating fluorescent materials with AIE properties into MOFs.[17–19] Compared with the complex designed organic linker, incorporating fluorescent materials exhibiting the AIE property into MOFs is a straightforward and effective method. Among these fluorescent

Department of Analytical Chemistry, School of Science, China Pharmaceutical University, Nanjing 211198, Jiangsu, P.R. China. E-mail: liaoshenghua@cpu.edu.cn

† Electronic supplementary information (ESI) available. See DOI: https://doi.org/10.1039/d4an01506a

materials incorporated into MOFs, metal nanoclusters (M NCs) exhibiting the AIE property possess unique chemical and optical properties such as strong photoluminescence, larger Stokes shifts, and good water solubility, making them ideal candidates.[20–23] Moreover, the porosity of MOFs not only restricts the intramolecular motions of surface ligands in M NCs *via* the spatial confinement effect to enhance the quantum yields of M NCs, but also selectively permits target analytes to access the channels of f-MOFs, thereby amplifying the sensing signals and improving the specificity of the f-MOFs-based sensors.

To date, various M NCs@MOFs have been successfully designed and prepared as fluorescent nanoprobes for the detection of metal ions,[24,25] gases,[26] small molecules,[27,28] and biogenetic materials,[29] among others.[30–32] For example, Yang and coworkers designed an enzyme-free sensor by encasing Cu NCs in ZIF-8 for fluorescent and smartphone detection of chlorpyrifos.[33] Niu *et al.* integrated the synthesized gold nanoclusters with Mn-MOF to sensitively detect AFB1.[34] To the best of our knowledge, there is a scarcity of reports on employing f-MOFs constructed from M NCs with the AIE property as a nanoprobe for the detection of small molecular drug formulations.

Felodipine, a commonly calcium channel blocker, is an effective drug that is used in treating hypertension. However, its abuse can lead to severe adverse effects such as bradycardia.[35] Therefore, it is crucial to develop an efficient and sensitive method for detecting felodipine. Herein, a novel fluorescent nanocomposite Cu NCs@ZIF-8 was designed and fabricated by incorporating copper nanoclusters (Cu NCs) with the AIE property into zeolite imidazolate frameworks (ZIF-8). Owing to the spatial confinement of ZIF-8 and the electrostatic interaction between the positively charged ZIF-8 and the negatively charged Cu NCs, the as-prepared Cu NCs@ZIF-8 exhibited strong red emission under the excitation of UV light at 380 nm. Furthermore, the fluorescence of Cu NCs@ZIF-8 was significantly quenched by felodipine *via* the mechanism of the inner-filtration effect. Thus, a novel fluorescence nanoprobe based on Cu NCs@ZIF-8 was constructed for detecting the labelling-amount percentage of felodipine tablets (as shown in Scheme 1). Experimental results demonstrated that our proposed nanoprobe exhibits favorable linear response, precision and accuracy.

Experimental section

Synthesis of Cu NCs with AIE property

Cu NCs with AIE property were synthesized according to previous work from our laboratory.[36] Typically, lipoic acid (0.6 mmol) and NaOH (40 mM, 15 ml) were introduced into a three-necked flask. Subsequently, the aforementioned solution was stirred for 30 minutes at room temperature. After sequentially adding $NaBH_4$ (0.5 mM, 5 ml) and $CuCl_2{\cdot}2H_2O$ (0.2 mM, 5 ml), the obtained mixture was adjusted to a pH of 13 by dropwise addition of NaOH (40 mM). The resulting solution was then stirred for another 3 hours, yielding a yellow solution. Finally, the Cu NCs product was obtained through vacuum drying.

Synthesis of the fluorescent nanocomposite Cu NCs@ZIF-8

The Cu NCs@ZIF-8 nanocomposites were prepared by following the reported literature with some necessary modifications.[37] Briefly, 10 mg of Cu NCs solid powder was dissolved in 4 mL of ultrapure water. After adding 150 mg of Zn $(NO_3)_2{\cdot}6H_2O$, the resulting mixture was stirred for 5 minutes at room temperature. Subsequently, 124 mg of 2-methylimidazole (2-MIM) dissolved in 7.5 mL of ultrapure water was added dropwise, followed by stirring for an additional 10 minutes to obtained the yellow color Cu NCs@ZIF-8 nanocomposite. After being washed and centrifuged three times with ethanol,

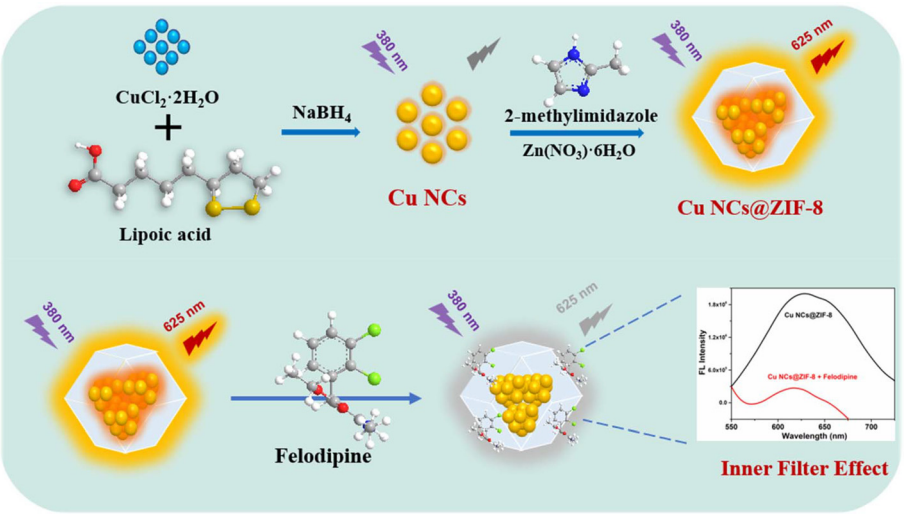

Scheme 1 Schematic illustrating the synthesis of Cu NCs@ZIF-8 and its application for the detection of felodipine.

the obtained Cu NCs@ZIF-8 powder was vacuum dried for further use.

The PL quantum yield of Cu NCs and Cu NCs@ZIF-8

The PL quantum yields of Cu NCs and Cu NCs@ZIF-8 were measured using a relative method, in which rhodamine B dissolved in ethanol (the quantum yield of 56%) was used as a reference. The quantum yields (QYs) of the Cu NCs and Cu NCs@ZIF-8 were calculated according to the following equation:

$$\Phi_x = \Phi_r \times \frac{A_r}{A_x} \times \frac{F_x}{F_r} \times \frac{{n_x}^2}{{n_r}^2}$$

where the subscripts "r" and "x" denote rhodamine B, Cu NCs or Cu NCs@ZIF-8, respectively, "Φ" represents the quantum yield, "A" indicates the absorbance, "F" represents the integrated areas of the fluorescent emission peak of rhodamine B, Cu NCs or Cu NCs@ZIF-8, and "n" is a refractive index of solvents.

Encapsulation efficiency of Cu NCs in ZIF-8

To investigate the encapsulation efficiency of Cu NCs in Cu NCs@ZIF-8, yellow Cu NCs@ZIF-8 nanocomposites were synthesized following the aforementioned method. The obtained Cu NCs@ZIF-8 were collected by centrifugation, followed by washing twice to remove the nonencapsulated Cu NCs. The amount of unencapsulated Cu NCs in the supernatant solution was measured using UV-Vis spectroscopy. Finally, the encapsulation efficiency (EE%) of Cu NCs was calculated according to the following equation:

$$\mathrm{EE}\% = \frac{\text{the weight of total Cu NCs} - \text{the weigth of free Cu NCs}}{\text{the weight of total Cu NCs}} \times 100\%.$$

Assaying the labelling-amount percentage of felodipine tablets using the nanoprobe based on Cu NCs@ZIF-8

A sample solution of felodipine was prepared as follows: 20 tablets of felodipine were ground into a fine powder. Then, an accurately weighed appropriate amount of felodipine powder (equivalent to 1.5 mg of felodipine) was dissolved with 10 mL PBS buffer (10 mM, pH = 8.5). After being filtrated by a 0.22 μm filtration membrane, the sample solution of felodipine (0.4 mM) was obtained. A standard solution of felodipine (0.4 mM) was prepared by dissolving an accurately weighed 1.5 mg of felodipine reference substance in 10 ml of PBS buffer (10 mM, pH = 8.5).

Subsequently, 50 μL of either the sample or standard solution was mixed with 100 μL of Cu NCs@ZIF-8 solution (5 mg ml^{-1}) and 850 μL of PBS buffer solution (10 mM, pH = 8.5). The fluorescence spectra of the mixtures were recorded with a fluorescence spectrophotometer under 380 nm wavelength excitation (both excitation and emission slits were set as 10 nm).

Results and discussion

Synthesis and characterization of Cu NCs and Cu NCs@ZIF-8

Cu NCs was prepared using $CuCl_2{\cdot}2H_2O$ and lipoic acid by chemical reduction method. The morphology of the resulting Cu NCs was examined through transmission electron microscopy (TEM) imaging. As demonstrated in Fig. 1A and B, the Cu NCs dispersed in aqueous solution appear as a regular spherical nanoparticle with a mean diameter of 3.1 ± 1.4 nm.

The morphology of the obtained Cu NCs@ZIF-8 nanocomposite was characterized using TEM. As can be seen in the TEM image of Fig. 1C, the uniformly dispersed Cu NCs aggregated in the presence of Zn^{2+}. The prepared Cu NCs@ZIF-8 had a regular rhombic dodecahedral morphology with an average particle size of around 60 nm (Fig. 1D), which was similar to that of ZIF-8 in previous reports.[38]

The crystalline Cu NCs@ZIF-8 was further analyzed with the help of XRD. As shown in Fig. 2A, the diffraction peaks in the XRD patterns of the prepared ZIF-8, Cu NCs@ZIF-8, are highly overlapped with those of the reported ZIF-8,[38] indicating that introducing Cu NCs into ZIF-8 had almost no effect on the crystallinity of ZIF-8. Moreover, the change in the zeta potential of ZIF-8 before and after incorporating Cu NCs also further proved that Cu NCs had been successfully encapsulated in ZIF-8 (Fig. 2B). The FT-IR spectrum of Cu NCs@ZIF-8 shows a stretching vibration peak of the Zn–O bond at 535 cm^{-1}, indicating that the coordination interaction between $-COO^-$ and Zn^{2+} plays important roles in the formation of Cu NCs@ZIF-8 (Fig. 2C).

The chemical elements and valence states of Cu NCs were analyzed using X-ray photoelectron spectroscopy (XPS). The XPS spectrum of Cu NCs@ZIF-8 exhibited six distinct peaks corresponding to C 1s, N 1s, O 1s, S 2p, Cu 2p and Zn 2p (Fig. 2D). As expected, the characteristic peaks of 2p3/2 and Cu 2p1/2 in the XPS spectrum of Cu NCs@ZIF-8 are located at 932.3 and 952.2 eV, respectively, demonstrating the absence of Cu(II) in the as-prepared Cu NCs@ZIF-8 (Fig. 2E).[26] Compared with the XPS spectrum of Cu NCs (Fig. S1†), the identical position of the Cu 2p characteristic peaks verified that ZIF-8 exclusively serves as a protective shell to encapsulate Cu NCs without causing a valence change or disrupting their intrinsic properties. The observed slight shift in the O 1s peak (from 531.08 eV to 531.88 eV) and the emergence of a new peak attributed to elemental Zn at 1020–1025 cm^{-1} in the XPS spectrum of Cu NCs@ZIF-8 provide further evidence supporting the existence of the coordination interaction between the $-COO^-$ groups in the surface ligands of Cu NCs and the second building units Zn^{2+} of ZIF-8 during the synthesis of Cu NCs@ZIF-8 (Fig. 2F).

The optical properties of Cu NCs@ZIF-8 were systematically characterized by UV-Vis absorption and fluorescence spectroscopy. As shown in Fig. 3A, there are no significant absorption peaks within the range of 250–350 nm in the absorption spectrum of ZIF-8, whereas Cu NCs@ZIF-8 displayed a shoulder peak that is analogous to that of Cu NCs. Meanwhile, the prepared Cu NCs@ZIF-8 solid powder emitted an obvious

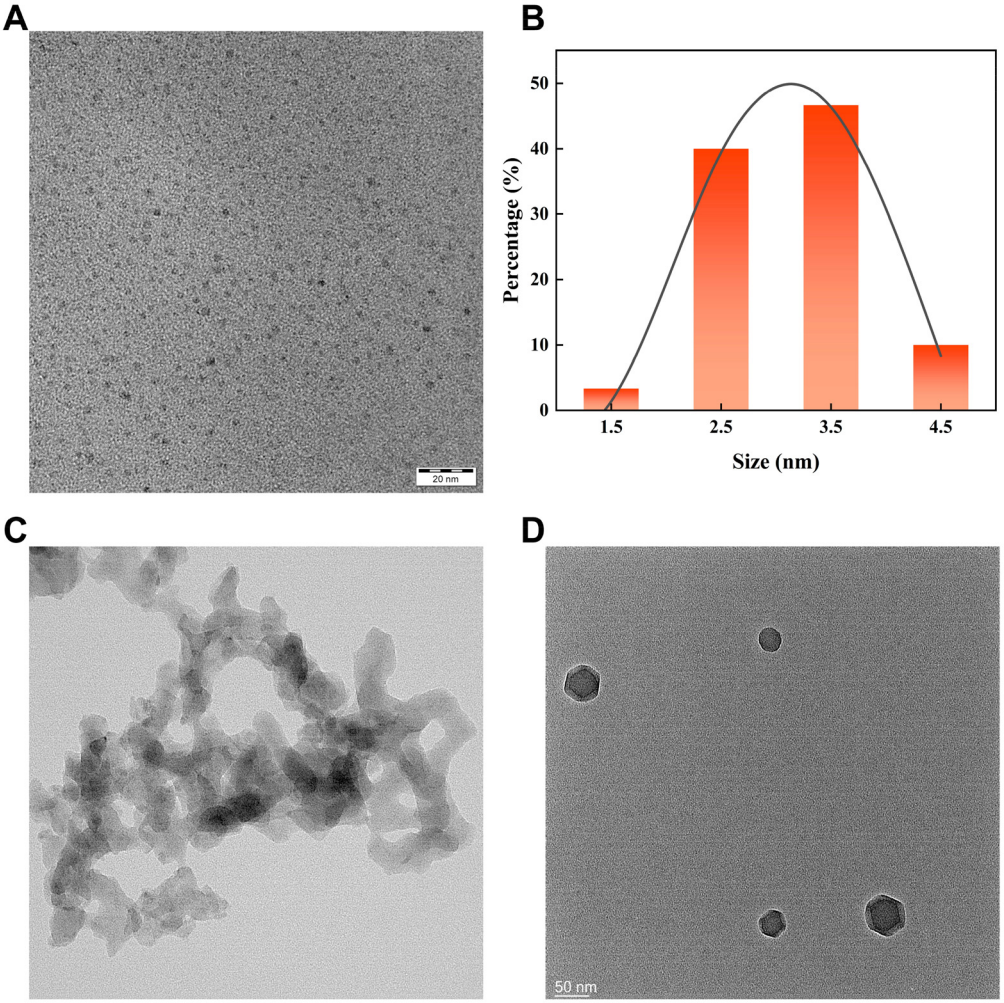

Fig. 1 (A) TEM image and the size distribution (B) of Cu NCs; (C) TEM image of Cu NCs + Zn^{2+}; (D) TEM image of Cu NCs@ZIF-8.

red fluorescence under excitation by an ultraviolet light of 365 nm (Fig. S2†). Additionally, the emission spectra of Cu NCs, ZIF-8, and Cu NCs@ZIF-8 in aqueous solution with the same concentration of 0.5 mg ml^{-1} were compared (Fig. 3B). The maximum emission wavelength of the Cu NCs@ZIF-8 aqueous solution is located at 625 nm, which presents a slight blue shift compared to that of the Cu NCs aqueous solution. The slight blue shift in the maximum emission wavelength of Cu NCs@ZIF-8 may have resulted from the spatial confinement of Cu NCs provided by ZIF-8 and the change in the electron distribution of Cu NCs *via* physical or chemical interaction, such as electrostatic interaction or coordination interaction. Notably, the fluorescence intensity of Cu NCs@ZIF-8 was significantly higher than that of Cu NCs. The photoluminescence quantum yield of Cu NCs or Cu NCs@ZIF-8 was measured as 12.57% and 41.69%, respectively. The enhanced photoluminescence quantum yield of Cu NCs@ZIF-8 can be attributed to the restricted intramolecular motion of the surface ligands in Cu NCs imposed by ZIF-8, thereby promoting the AIE effect. As depicted in Fig. S3,† the fluorescent intensity of the Cu NCs@ZIF-8 powder stored in a desiccator shows a negligible decrease over a period of 7 days. There is no significant change in the fluorescence intensity of the Cu NCs@ZIF-8 aqueous solution for up to 12 h (Fig. S4†). These experimental results demonstrated that the fluorescence intensity of the Cu NCs@ZIF-8 powder and Cu NCs@ZIF-8 aqueous solution present good stability. Finally, the encapsulation efficiency of Cu NCs in Cu NCs@ZIF-8 was measured to be 29.65% by UV-Vis spectroscopy.

In summary, these experimental results demonstrate that encapsulating Cu NCs with the property of AIE within ZIF-8 enables the fabrication of the fluorescent nanocomposite Cu NCs@ZIF-8 without altering the intrinsic characteristics of Cu NCs and ZIF-8.

Fluorescence quenching of Cu NCs@ZIF-8 caused by felodipine

The remarkable fluorescence properties and excellent aqueous stability of Cu NCs@ZIF-8 prompted us to investigate its potential application in the sensing of small molecular drugs. As a

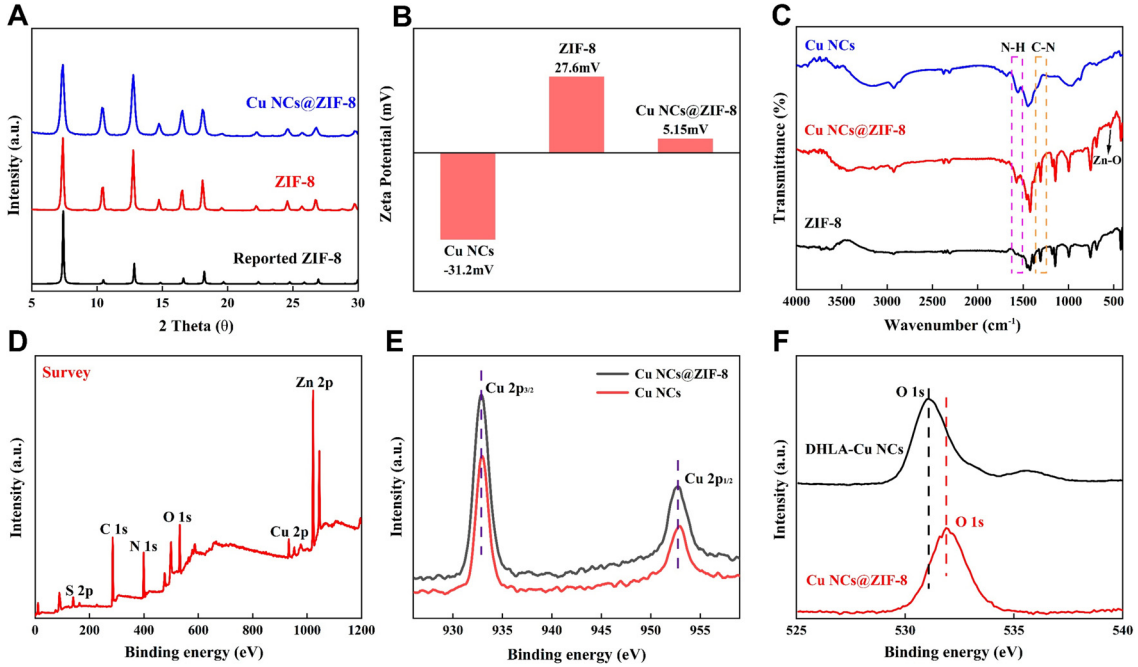

Fig. 2 (A) XRD spectrum of ZIF-8 and Cu NCs@ZIF-8; (B) zeta potential of Cu NCs, ZIF-8 and Cu NCs@ZIF-8; (C) FTIR spectrum of ZIF-8, Cu NCs and Cu NCs@ZIF-8; (D) survey XPS spectrum of Cu NCs@ZIF-8; (E) XPS spectrum of the Cu 2p region in Cu NCs and Cu NCs@ZIF-8; (F) XPS spectrum of the O 1s region in Cu NCs and Cu NCs@ZIF-8.

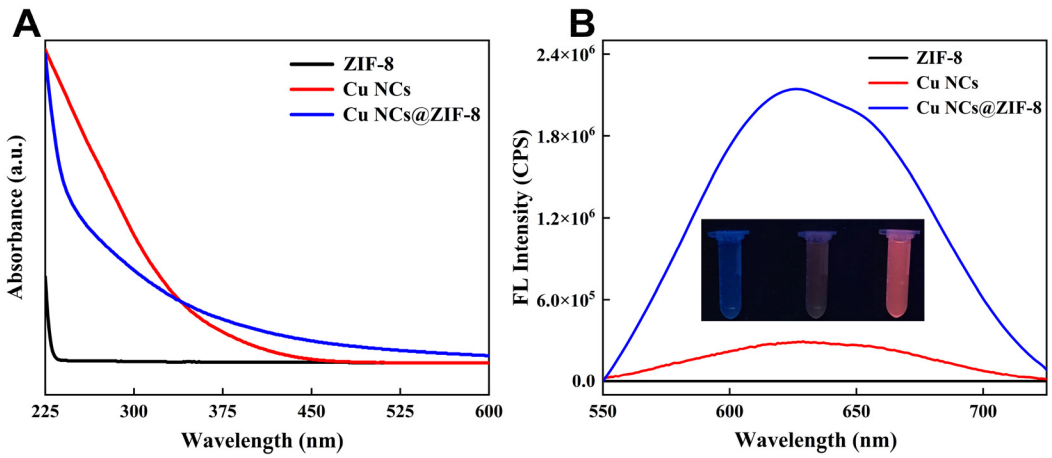

Fig. 3 (A) UV absorption of ZIF-8, Cu NCs and Cu NCs@ZIF-8; (B) fluorescence emission spectra of ZIF-8, Cu NCs and Cu NCs@ZIF-8 (inset: the pictures of ZIF-8, Cu NCs and Cu NCs@ZIF-8 aqueous solution under UV light of 365 nm from left to right).

common drug for treating hypertension, the misuse of felodipine can result in severe adverse effects, such as bradycardia.[35] Therefore, it is crucial for ensuring the quality control and therapeutic efficacy of felodipine tablets to accurately determine the labelling-amount percentage. As illustrated in Fig. 4A, the fluorescence intensity of Cu NCs@ZIF-8 was significantly quenched upon introducing felodipine. To investigate the fluorescence quenching mechanism of Cu NCs@ZIF-8 by felodipine, we first compared the UV-Vis absorption spectrum of felodipine with the excitation and emission spectra of Cu NCs@ZIF-8. As depicted in Fig. 4B, a distinct absorption peak appeared at 360 nm in the UV-Vis absorption spectrum of felodipine. The maximal excitation and emission wavelengths of Cu NCs@ZIF-8 were located at 380 nm and 625 nm, respectively. There is a significant overlap between the UV-Vis absorption spectrum of felodipine and the excitation spectrum of Cu NCs@ZIF-8. Therefore, it can be rationally inferred that the fluorescence quenching of Cu NCs@ZIF-8 by felodipine resulted from the inner-filtration effect.

In general, the fluorescence lifetime of fluorophores can provide information about the decay kinetics of electrons in the excited state.[39–42] Therefore, the fluorescence lifetimes of

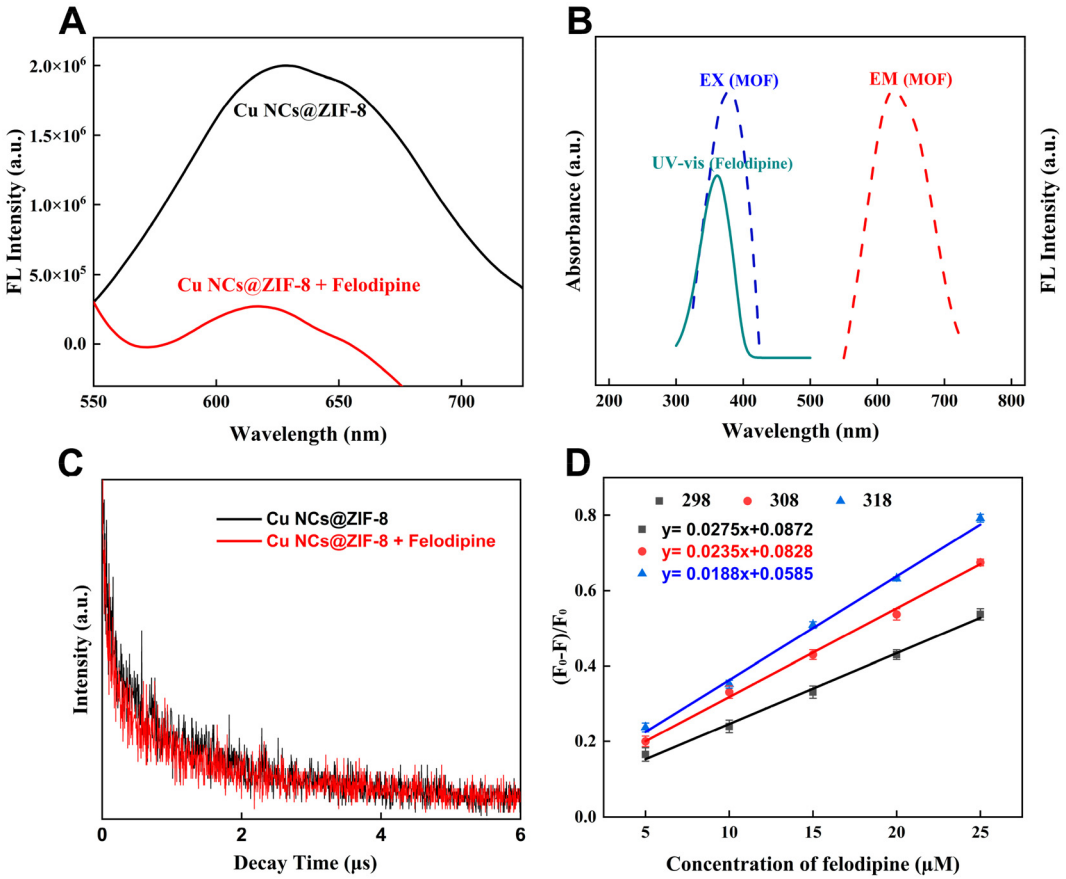

Fig. 4 (A) The fluorescence spectra of Cu NCs@ZIF-8 with (red) and without felodipine (black); (B) UV absorption spectrum of felodipine and the excitation and emission spectra of Cu NCs@ZIF-8; (C) fluorescence lifetimes of Cu NCs@ZIF-8 with (red) and without felodipine (black); (D) the Stern–Volmer plots of Cu NCs@ZIF-8 in the presence of different concentrations of felodipine at 298, 308, and 318 K.

the Cu NCs@ZIF-8 nanocomposite before and after adding felodipine were measured by time-solved fluorescence spectroscopy. As demonstrated in Fig. 4C, the photoluminescence lifetime of Cu NCs@ZIF-8 in the presence of felodipine is 0.705 μs, consistent with the photoluminescence lifetime (0.706 μs) of merely Cu NCs@ZIF-8, indicating that the fluorescence quenching of Cu NCs@ZIF-8 by felodipine is not caused by the change in the excited state of Cu NCs@ZIF-8. The Stern–Volmer equation was utilized to validate the quenching mechanism of Cu NCs@ZIF-8 by felodipine. The expression of the Stern–Volmer equation is described as follows:

$$\frac{F_0}{F} = 1 + K_{SV}[Q]$$

where F_0 and F represent the fluorescence emission of Cu NCs@ZIF-8 before and after the addition of felodipine, respectively, K_{SV} denotes the quenching constant, and Q signifies the concentration of felodipine. As shown in Fig. 4D, the quenching constant (slope) decreases with increasing temperatures, indicating that the fluorescence quenching of Cu NCs@ZIF-8 by felodipine is ascribed to the mechanism of static quenching.

Performance evaluation of CS-Cu NCs nanoprobes for assaying felodipine

The performances of our proposed nanoprobe based on Cu NCs@ZIF for assaying felodipine were evaluated under optimal conditions (Fig. S5†). As shown in Fig. 5A, the fluorescence intensity of Cu NCs@ZIF-8 gradually decreased as the concentration of felodipine was gradually increased from 1 μM to 25 μM. The $(F_0 - F)/F_0$ of Cu NCs@ZIF-8 in the absence or presence of felodipine presented a good linear relationship with the concentration of felodipine, in which F or F_0 represents the fluorescence intensity of Cu NCs@ZIF-8 with or without felodipine, respectively (Fig. 5B). The limit of detection (LOD) for felodipine of our proposed novel Cu NCs@ZIF-8 nanoprobe was calculated as 0.09 μM according to the $3\delta/s$ method, where "δ" is the relative standard deviation of the fluorescence intensity of the blank solution and s is the slope of the linear regression equation. Compared to most of the reported methods, the proposed Cu NCs@ZIF-8 nanoprobe in this work had a lower LOD (Table 1).

Then, the repeatability of the novel Cu NCs@ZIF-8-based nanoprobe for the assaying of felodipine was also verified. As depicted in Fig. 5C, the relative standard deviation (RSD) of

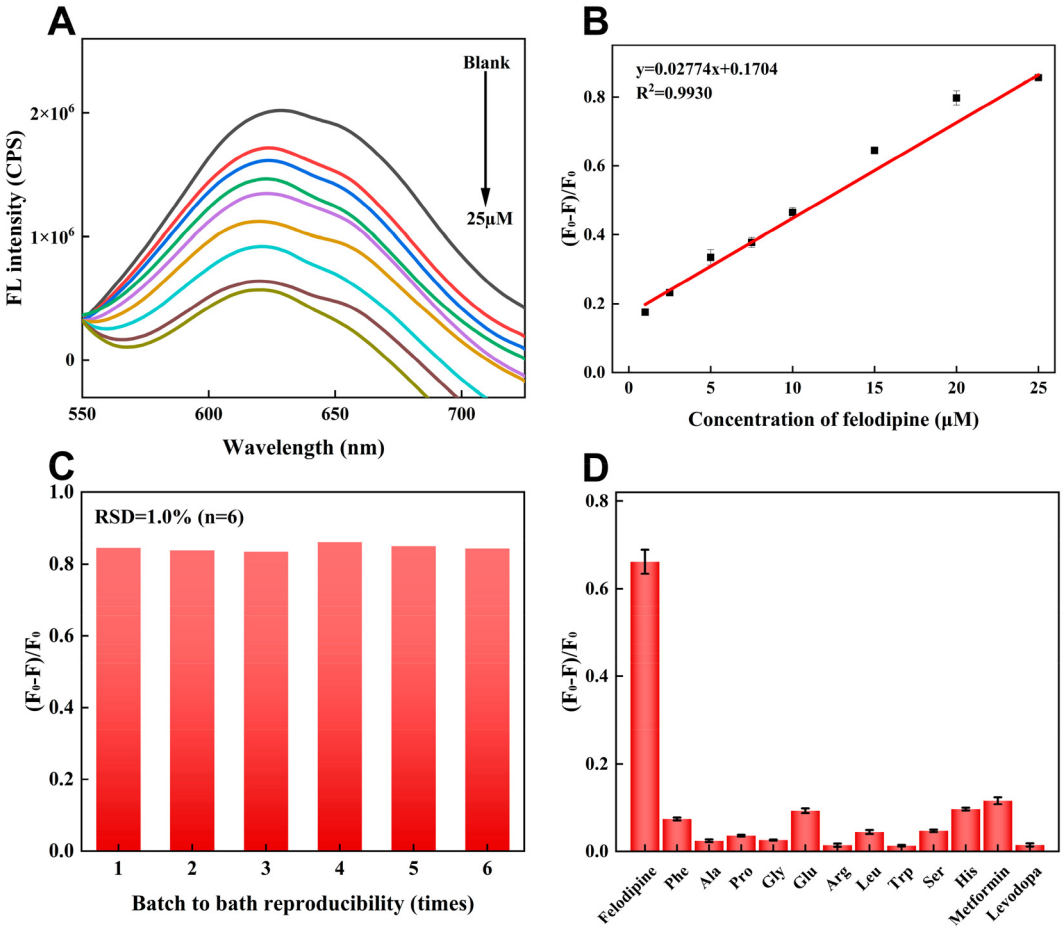

Fig. 5 (A) Fluorescence spectra of Cu NCs@ZIF-8 in the presence of felodipine ranging from 1 to 25 μM; (B) the regression curve of $(F_0 - F)/F_0$ of Cu NCs@ZIF-8 *versus* the concentration of felodipine; (C) reproducibility of $(F_0 - F)/F_0$ of the mixed system, consistent with Cu NCs@ZIF-8 and felodipine; (D) the $(F_0 - F)/F_0$ of Cu NCs@ZIF-8 before and after adding felodipine in the presence of various interfering substances.

Table 1 Comparison of Cu NCs@ZIF-8 with previous methods used for felodipine determination

Sensors	Method	Linear range (μM)	LOD (μM)	Ref.
Fe(III)/Fe(II)	Spectrophotometric	3.9–13	2.80	43
Nanoparticles	Fluorescent	0.1–0.5	6.4×10^{-3}	44
—	MES	0.5–10.5	0.13	45
—	RP-HPLC	0.65–52	0.14	46
Cu NCs@ZIF-8	Fluorescent	1–20	0.09	This work

CPE: carbon paste electrode; SDS: sodium dodecyl sulfate; DPSV: differential pulse voltammetry; MES: micelle-enhanced spectrofluorimetric; RP-HPLC: reverse phase high-performance liquid chromatographic.

the $(F_0 - F)/F_0$ of Cu NCs@ZIF-8 in the presence or absence of felodipine was determined to be 1.0% (n = 6). This result indicated that the Cu NCs@ZIF-8 nanoprobe presents good repeatability in assaying felodipine. Moreover, the selectivity of the Cu NCs@ZIF-8 nanoprobe for felodipine was also evaluated. In the presence of 250 μM of interference substances, including the common amino acids (phenylalanine, alanine, proline, glycine, glutamic acid, arginine, leucine, tryptophan, serine, histidine), mercaptan drugs such as metformin, and levodopa, there is no obvious impact on the determination of 25 μM of felodipine by our proposed Cu NCs@ZIF-8 nanoprobe (Fig. 5D). Meanwhile, the existence of common interfering metal ions and anion ions (such as Na^+, K^+, Ca^{2+}, Mg^{2+}, Cd^{2+}, Mn^{2+}, NH_4^+, Zn^{2+}, Sr^{2+}, Cl^-, Br^-, I^-, CO_3^{2-}, HCO_3^- and SO_4^{2-}) have a negligible impact on $(F_0 - F)/F_0$ of Cu NCs@ZIF-8 (Fig. S6†).

To validate the feasibility of the Cu NCs@ZIF-8 nanoprobe in practical application, the labelling-amount percentage of commercially available felodipine tablets was measured. As shown in Table S1,† the mean labelling-amount percentage of felodipine tablets was calculated to be 102.6% with an RSD of 1.5% (n = 6) from six parallel measurements. Meanwhile, the labelling-amount percentage of the felodipine tablets was determined to be 99.42% (RSD = 1.4%, n = 6) by a high-performance liquid chromatography (HPLC) method adopted from Chinese Pharmacopoeia (Table S2†). This is consistent with the result measured by our proposed method. Finally, the accuracy of Cu

NCs@ZIF-8 for assaying felodipine was validated by spiked sample experiment. The measured recovery of Cu NCs@ZIF-8 for felodipine at three different concentration levels ranged from 99.71% to 102.9% with a relative average deviation (RAD) of less than 4.0% (n = 3), confirming that our proposed Cu NCs@ZIF-8 exhibits excellent accuracy (Table S3†).

Conclusion

In conclusion, a facile aqueous-phase approach was proposed for synthesizing the highly fluorescent emission nanocomposite Cu NCs@ZIF-8 in this paper. Attributed to the AIE of Cu NCs and the spatial confinement provided by ZIF-8, the as-prepared Cu NCs@ZIF-8 emitted bright red fluorescence under the excitation light of 380 nm, whereas there is no observable fluorescence emission in the pure Cu NCs aqueous solution. Owing to the overlap between the UV-Vis absorption spectrum of felodipine and the excitation spectrum of Cu NCs@ZIF-8, a novel Cu NCs@ZIF-8 nanoprobe was designed to determine the labelling-amount percentage of commercially available felodipine tablets. Experimental results confirmed that our proposed Cu NCs@ZIF-8 nanoprobe exhibits high sensitivity, a good linear response range, and excellent accuracy, thereby enriching the application of fluorescent MOFs-based nanocomposites encapsulating metal nanoclusters with AIE property in pharmaceutical quality control.

Author contributions

Juan Du: conceptualization, formal analysis, writing – original draft preparation. Huixiao Tong: picture processing. Jinwen Chen: draft revising. Qikun Zhang: conceptualization and draft revising. Shenghua Liao: conceptualization, writing – review & editing, funding acquisition.

Data availability

The data that support the findings of this study are available from the corresponding author upon reasonable request.

Conflicts of interest

There are no conflicts to declare.

References

1 C. Gu, Z. Yu, J. Liu and D. S. Sholl, *ACS Appl. Mater. Interfaces*, 2021, **13**, 11039–11049.
2 M. A. Gordillo, P. A. Benavides, K. Ma and S. Saha, *ACS Appl. Nano Mater.*, 2022, **5**, 13912–13920.
3 B. Mohanty, S. Kumari, P. Yadav, P. Kanoo and A. Chakraborty, *Coord. Chem. Rev.*, 2024, **519**, 216102.
4 B. Szczesniak, J. Choma and M. Jaroniec, *J. Colloid Interface Sci.*, 2018, **514**, 801–813.
5 X. Li and Q.-L. Zhu, *EnergyChem*, 2020, **2**, 100033.
6 Y. Liu, X.-Y. Xie, C. Cheng, Z.-S. Shao and H.-S. Wang, *J. Mater. Chem. C*, 2019, **7**, 10743–10763.
7 T. K. Pal, *Mater. Chem. Front.*, 2023, **7**, 405–441.
8 W. Fan, H. Chang, J. Zhong, J. Lu, G. Ma, H. Zhang, Z. Jiang and G. Yin, *Sep. Purif. Technol.*, 2024, **330**, 125258.
9 S. Bazazi, E. Hashemi, M. Mohammadjavadi, M. R. Saeb, Y. Liu, Y. Huang, H. Xiao and F. Seidi, *Adv. Colloid Interface Sci.*, 2024, **328**, 103178.
10 J. Du, T. Jia, F. Li, Y. Li, Q. Wang, L. He, H. Ågren and G. Chen, *Adv. Funct. Mater.*, 2024, 2401272, DOI: **10.1002/adfm.202401272**.
11 Q. Wei, S. Xue, W. Wu, S. Liu, S. Li, C. Zhang and S. Jiang, *Chem. Rec.*, 2023, **23**, e202200263.
12 V. Somjit, C. Kaiyasuan, P. Thinsoongnoen, T. Pila, V. Promarak and K. Kongpatpanich, *Microporous Mesoporous Mater.*, 2021, **328**, 111452.
13 M. Asad, M. I. Anwar, A. Abbas, A. Younas, S. Hussain, R. Gao, L.-K. Li, M. Shahid and S. Khan, *Coord. Chem. Rev.*, 2022, **463**, 214539.
14 Y. Jia, X. Zhang, J. Fang, D. Jia, T. Tian, Y. Du, Q. Wei and F. Li, *Biosens. Bioelectron.*, 2024, **264**, 116690.
15 Y. Jia, X. Zhang, X. Kuang, D. Fan, X. Sun, X. Ren, H. Ma, D. Wu and Q. Wei, *Anal. Chem.*, 2024, **96**, 12593–12597.
16 X. Zhai, Y. Kou, L. Liang, P. Liang, P. Su and Y. Tang, *Inorg. Chem.*, 2023, **62**, 18533–18542.
17 L. Zhang, X. Bi, H. Wang, L. Li and T. You, *Talanta*, 2024, **273**, 125843.
18 Z. Lu, M. Wu, S. Wu, S. Yang, Y. Li, X. Liu, L. Zheng, Q. Cao and Z. Ding, *Nanoscale*, 2016, **8**, 17489–17495.
19 H. Q. Yin, X. Y. Wang and X. B. Yin, *J. Am. Chem. Soc.*, 2019, **141**, 15166–15173.
20 D. Bain, S. Maity and A. Patra, *Chem. Commun.*, 2020, **56**, 9292–9295.
21 H. Zhu, S. Wang, Y. Wang, C. Song, Q. Yao, X. Yuan and J. Xie, *Biomaterials*, 2022, **288**, 121695.
22 X. Wei, X. Kang, S. Jin, S. Wang and M. Zhu, *CCS Chem.*, 2021, **3**, 1929–1939.
23 J. Zhao, Y. Lu, X. Zhang, Q. Liao, A. Tan, X. Ma and Y. Liu, *ACS Sustainable Chem. Eng.*, 2023, **11**, 13896–13906.
24 R. Zhao, W. Lu, X. Chai, C. Dong, S. Shuang and Y. Guo, *Anal. Chim. Acta*, 2024, **1298**, 342403.
25 X. Bi, L. Li, Q. Niu, X. Liu, L. Luo, H. Jiang and T. You, *Inorg. Chem.*, 2023, **62**, 3123–3133.
26 Z. H. Zhu, Z. Ni, H. H. Zou, G. Feng and B. Z. Tang, *Adv. Funct. Mater.*, 2021, **31**, 2106925.
27 Y. Zhang, Q. Lin, Y. Song, J. Huang, M. Chen, R. Ouyang, S.-Y. Liu and Z. Dai, *Chemosensors*, 2023, **11**, 429.
28 X. Hu, X. Liu, X. Zhang, H. Chai and Y. Huang, *Biosens. Bioelectron.*, 2018, **105**, 65–70.
29 C. S. Gujja and S. D. Pawar, *J. Inorg. Organomet. Polym. Mater.*, 2023, **33**, 2636–2646.
30 M. Wang, M. Hu, Z. Li, L. He, Y. Song, Q. Jia, Z. Zhang and M. Du, *Biosens. Bioelectron.*, 2019, **142**, 111536.

31 M. V. Varsha and G. Nageswaran, *Microchem. J.*, 2023, **188**, 108481.
32 Z. Wang, R. Chen, Y. Xiong, K. Cepe, J. Schneider, R. Zboril, C. S. Lee and A. L. Rogach, *Part. Part. Syst. Charact.*, 2017, **34**, 1700029.
33 F. Yang, S. Li, J. Ma and Q. Jia, *J. Food Compos. Anal.*, 2024, **135**, 106685.
34 X. Niu, Z. Suo, J. Li, M. Wei, H. Jin and B. He, *Chem. Eng. J.*, 2024, **479**, 147806.
35 J. K. Geroge, P. R. P. Verma, J. Venkatesan, J. Y. Lee, D. H. Yoon, S. K. Kim and S. K. Singh, *AAPS PharmSciTech*, 2017, **18**, 2871–2888.
36 Q. Zhang, J. Duan, J. Chen, J. Du, H. Tong and S. Liao, *J. Fluoresc.*, 2024, 10895, DOI: **10.1007/s10895-024-03701-0**.
37 N. Zhu, K. Yuan, D. Xiong, F. Ai, K. Zeng, B. Zhao, Z. Zhang and H. Zhao, *Chem. Eng. J.*, 2023, **462**, 142129.
38 G. Zheng, Z. Chen, K. Sentosun, I. Perez-Juste, S. Bals, L. M. Liz-Marzan, I. Pastoriza-Santos, J. Perez-Juste and M. Hong, *Nanoscale*, 2017, **9**, 16645–16651.
39 J. S. Jang, H. L. Lee, K. H. Lee, J. Y. Lee and W. P. Hong, *J. Mater. Chem. C*, 2021, **9**, 2408–2415.
40 Z. Han, K. Wang, Y. Chen, J. Li, S. J. Teat, S. Yang, W. Shi and P. Cheng, *CCS Chem.*, 2022, **4**, 3238–3245.
41 H. Min, Z. Han, T. Sun, K. Wang, J. Xu, P. Yao, S. Yang, P. Cheng and W. Shi, *Sci. China: Chem.*, 2023, **66**, 3511–3517.
42 M. Wang, Z. Han, K. Wang, B. Zhao, T. Sun, Y. Wu, P. Cheng and W. Shi, *Angew. Chem., Int. Ed.*, 2023, **63**, e20231872.
43 K. Basavaiah, U. Chandrashekar and H. C. Prameela, *Farmaco*, 2003, **58**, 141–148.
44 Y. P. Jiang, X. H. Fang, Q. Wang, J. Z. Huo, Y. Y. Liu, X. R. Wang and B. Ding, *Commun. Chem.*, 2023, **6**, 96.
45 M. I. Walash, F. F. Belal, N. M. El-Enany and M. H. El-Maghrabey, *BMC Chem.*, 2011, 35516.
46 A. M. Mohamed, M. A. Omar, M. A. Hammad and A. A. Mohamed, *Spectrochim. Acta, Part A*, 2015, **149**, 934–940.